Control of the production of highly charged ions in femtosecond-laser cluster fragmentation

S. Zamith, T. Martchenko, Y. Ni, S. A. Aseyev, H. G. Muller, and M. J. J. Vrakking

FOM Institute for Atomic and Molecular Physics (AMOLF), Kruislaan 407, 1098 SJ Amsterdam, The Netherlands

We present the results of optimal-control experiments and calculations on the production of highly charged ions in intense laser field irradiation of large xenon clusters. Experimentally, a spectacular enhancement in the yield of highly charged ions is observed when clusters are subjected to an optimized laser field consisting of a sequence of two pulses, with a time delay that depends on the intensity of the laser and the size of the clusters. Similar results are obtained in optimal-control calculations, which demonstrate that the optimized pulse shape maximizes the efficiency of resonant heating.

PACS number(s): 36.40.Gk, 52.50.Jm

The interaction of clusters with high-intensity lasers has received much attention in the last few years. Clusters represent a laser target with a density close to that of a solid, where nearly 100% of the incoming light can be absorbed [1], without the possibility for relaxation of the deposited energy into bulk material. Hence, they are ideal targets for the production of energetic particles. Cluster explosions lead to the production of very energetic (MeV) and highly charged ions [2], keV electrons and soft x-ray photons, the latter being a candidate for use in euv lithography. The irradiation of deuterium clusters with intense femtosecond laser can even lead to nuclear fusion [3].

Various models [4–7] have been developed to explain the production of energetic particles in cluster explosions. Common to these models, individual atoms are ionized via tunnel ionization when the laser reaches a high enough intensity, leading to a charge build-up in the cluster. Further ionization occurs via electron impact ionization and field ionization (assisted by the proximity of positive ions). In models for small clusters [6] (up to 30 atoms/cluster) resonance effects related to enhanced ionization at a critical atomic internuclear separation have been predicted, similar to the process of multi-electron dissociative ionization (MEDI) in diatomic molecules, while in the nanoplasma model [7] for large clusters the laser-cluster coupling is enhanced when the plasma is resonantly heated at the moment that the density of free electrons becomes equal to 3 times the critical density n_{crit}. Support for the nanoplasma model has come from measurements of ion kinetic energy and charge-state distributions as a function of pulse duration [8], and—in particular—electron kinetic energy distributions [9] which showed "warm" electrons with energies up to 2 keV and a sharp "hot electron" peak attributed to electrons that leave the cluster at the resonant heating point where the electron density n_e drops to $3n_{crit}$. Very recently, the applicability of the nanoplasma model to finite size cluster systems has been questioned, however, following a number of reports [10,11] that were unable to reproduce the results of Refs. [9–11]. In the present paper we present an experimental optimization of the production of highly charged ions resulting from the interaction of an intense laser field with large xenon clusters using an optimal-control [12] approach. Tailored laser pulses were applied and the production of highly charged ions was used as a diagnostic for the laser-cluster coupling efficiency. We find

an optimal pulse shape that reveals resonant heating as predicted by models like the nanoplasma model, and furthermore report optimal-control calculations that lead to optimized pulse shapes similar to those seen in the experiment.

In the experiment the rare gas clusters were produced in a differentially pumped vacuum system. The gas was expanded through a $\phi = 500$-μm pulsed nozzle (50 Hz repetition rate). Using the Hagena parameter [13] the average number of atoms in the clusters is estimated to be $\langle N \rangle \approx 1.6 \times 10^4$ with a standard supersonic nozzle and $\langle N \rangle \approx 2 \times 10^6$ with a conical nozzle, using 6 bars of xenon backing pressure. The high-intensity laser was a chirped-pulse amplification (CPA) system. After compression 100 fs, 230 μJoule pulses were produced, at a repetition rate of 1 kHz, and with a central wavelength of 800 nm. The laser beam was focused with a 150-mm focal-length lens ($f/D = 7.5$). The intensity at the cluster beam was estimated to be 5×10^{15} W/cm^2. Before amplification the pulses were sent through a $4f$ arrangement with a Spatial Light Modulator (SLM, Jenoptik, SLM-S 640/12) in the Fourier plane. The SLM consists of 640 independent strips, to which voltages were applied (with 12-bit resolution), in order to apply phase shifts $\phi(\omega)$ to the different spectral components of the pulse. Different phase patterns lead to different temporal pulse shapes, according to the Fourier transform relation $E(t) = \int E(\omega)e^{i\omega t}d\omega$, where $E(\omega) = |E(\omega)|e^{i\phi(\omega)}$ is the laser field in the frequency domain and $\phi(\omega)$ the phase applied with the SLM. The spectral range covered by the SLM was centered at 800 nm and extended over 100 nm. The parameters describing the laser field were varied in an automated way, in order to find the optimum pulse shape for the production of highly charged ions.

Ions were detected using a velocity-map imaging set-up [14] that was used as a simple time-of-flight (TOF) spectrometer without making use of its imaging capabilities. The ions were accelerated towards a dual microchannel plate (MCP) and the repeller and extractor electrode voltages (5.21 kV and 4.31 kV on the repeller and extractor electrodes) were adjusted in order to have as good a TOF resolution as possible. The TOF traces were recorded with a 0.5 GHz oscilloscope. We note that the experimental arrangement allowed photons and fast electrons to be observed as well.

Figure 1(a) shows a typical TOF trace that was obtained when xenon clusters with an average size $\langle N \rangle \approx 1.6 \times 10^4$
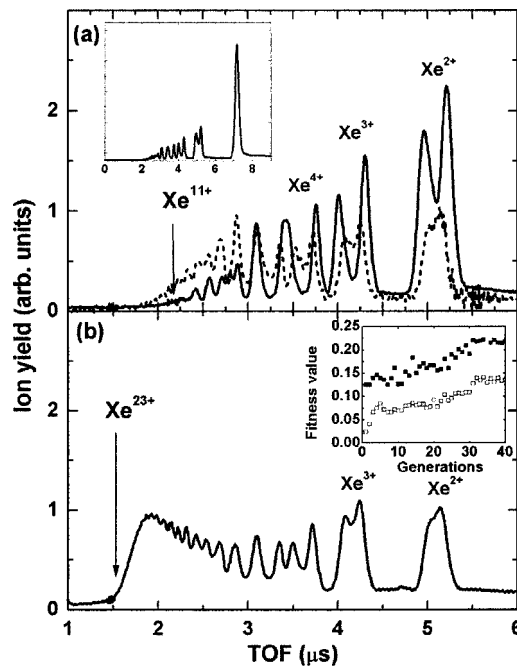
FIG. 1. Time-of-flight (TOF) traces for the interaction of xenon clusters $[\langle N \rangle \approx 1.6 \times 10^4$ (a)] with a Fourier-transform-limited 100 fs, 800 nm, 10^{15} W cm^{-2} laser pulse (N.B. The inset shows the complete TOF trace) (solid line) and the optimal linearly chirped laser pulse (dashed line) for forming highly charged ions derived from the former ($\sim$500 fs long); (b) with the optimum pulse shape obtained by means of an 80-parameter unrestricted optimization. As shown in Fig. 2(a) the optimum pulse consists of a sequence of two 120 fs pulses, separated by 500 fs. The inset in (b) shows the evolution of the fitness value for the 80-parameter optimization (full squares, maximum fitness; open squares, average fitness).

were irradiated with a nearly Fourier transform limited (FTL) 100 fs, 230 μJ pulse. All the peaks are quite broad due to the kinetic energy release in the laser-cluster interaction. For several charge states, ions emitted towards and away from the detector can be distinguished. No dependence of the shape of these peaks on the laser polarization axis was observed, which indicates that the ions were emitted isotropically. The forward and backward peaks are seen separately since due to their kinetic energy not all ions were collected on the detector and ions with a very large transverse velocity miss the detector. The maximum charge-state observed using the FTL pulse was Xe^{11+}. Extremely efficient coupling of the laser field to the cluster is responsible for the production of these highly charged states. When no clusters were present, the maximum observed charged state was Xe^{4+} under the same experimental laser conditions.

The optimal-control experiment consisted of enhancing the production of Xe^{n+}, with $n > 11$, with the help of a Simple Genetic Algorithm (SGA) [15]. Briefly, the SGA started with a random population of 50 individuals, with each individual representing a string of bits encoding the voltages on the SLM. In the present experiment the voltages applied across the SLM were varied in blocks of 5 pixels over a range of 400 pixels, so the search space consisted of 80 parameters. This way, every individual corresponded to a

specific phase pattern applied across the spectrum, with a corresponding different temporal pulse shape. All the individuals were assigned a fitness value by integrating the part of the TOF trace corresponding to the formation of highly charged states ($n > 11$) using a boxcar integrator. These individuals then underwent selection, according to their fitness. We used elitism for the 4 best individuals, uniform crossover ($P_c = 60\%$) and mutation ($P_m = 1\%$) to create a new generation, again consisting of 50 individuals, which were in turn experimentally tested [15]. As shown in the inset in Fig. 1(b) the average fitness increased until convergence was achieved. The solid curve in Fig. 1(b) shows the result of the optimization after 40 generations. A dramatic change in the charge-state distribution is observed, with a strong decrease in the lowest charge-states, and an increase in the highest charge-states up to 23+, compared to 11+ before the optimization. One should note that Xe^{10+} and Xe^{11+} are of particular importance for the generation of soft x rays in the $11-13.5$ nm range [16], where EUV lithography is developed.

One could argue that the optimized fitness involves not only the yield of highly charged ions but also the detection efficiency of these ions (since by lowering their kinetic energy the detection efficiency of the ions may be increased). We note however, that the current optimization also led to an increase in the total electron yield, whereas the ion yield for the lower charge-states substantially decreased (even though the kinetic energy for these charge-states decreased). Also, based on earlier work using linearly chirped laser pulses, one might suspect that the optimization simply consisted of applying an appropriate chirp to the pulse [17]. However, the results shown in Fig. 1(b) show substantially higher charge-states than the best (500 fs long) linearly chirped laser pulse that we could apply [the dashed line in Fig. 1(a).

To interpret the experimental results, the pulse shape leading to the optimal result was determined. The autocorrelation of the optimum pulse shape shown in Fig. 2(a), suggests that this pulse consists of a sequence of two $\sim$120 fs pulses with a similar amplitude and separated in time by $\sim$500 fs. Evidently there exists a specific time after triggering the cluster explosion when the coupling between the laser field and the cluster is maximal, and the optimization determines the optimum value of this time delay. We note that the peak intensity in the optimal pulse is only half of the peak intensity of the FTL pulse. Nevertheless, the production of highly charged atoms is strongly enhanced. It should be emphasized that the fact that the optimum pulse shape consists of a sequence of two pulses *does not* mean that the optimal-control experiment performed here was simply a pump-probe experiment. The experiment was an 80 parameter unbiased optimization proving that the formation of a sequence of two pulses and the existence of a specific delay between these two pulses are essential features of the optimization of laser-cluster interactions; very different pulse shapes could have been found if the physics of the problem had required this.

In order to elucidate the origin of the optimum pulse shape found in the experiment, a numerical pulse shaping experiment was performed on a computer, using a molecular dynamics simulation of the laser-cluster interaction [18]. Calculations were performed where small Xe clusters (N up
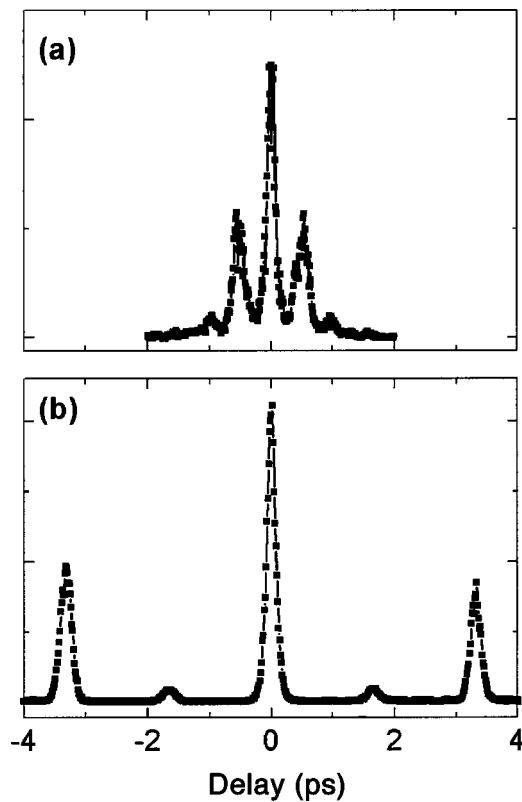
FIG. 2. Autocorrelation traces for pulses obtained by (a) an unrestricted 80-parameter optimization for $\langle N \rangle \approx 1.6 \times 10^4$ [Fig. 1(b)], and (b) a restricted 3-parameter optimization with larger clusters ($\langle N \rangle \approx 2.0 \times 10^6$). In the latter case the 3 parameters in the optimization were the amplitude and period of an oscillatory phase pattern applied to the LCD mask (leading to the formation of a pulse train) and the linear chirp of the pulse.

to 5056) interacted with a tailored laser field (derived from a 30 fs 3.5×10^{14} W/cm^2 Fourier-limited pulse). In these calculation atoms in the cluster ionized as a result of both field ionization and collisional ionization and trajectories of the ions and electrons were calculated from Newton's equations. The average ionic charge-state at the end of the laser-cluster interaction was used as fitness parameter for a genetic algorithm optimization, which in this case employed a population of 30 individuals and used 40 parameters to represent the phase function of the laser pulse. In Fig. 3(a) the optimized result is shown for Xe clusters consisting of 108 atoms/cluster. Similar to the experimental results, the optimum pulse consists of a pulse sequence where for this combination of cluster size and laser intensity the delay between the first and second pulse is equal to 146 fs. We note that the third pulse in Fig. 3(a) is a necessary by-product of the specification of the pulse in the spectral domain, and does not contribute to the ionization of the cluster.

Having observed that a two-pulse sequence optimizes the production of highly-charged ions experimentally using clusters of 1.6×10^4 atoms and numerically in calculations for clusters consisting of 108 atoms, the ionization dynamics of clusters with $N = 64$–5056 were numerically evaluated for two-pulse sequences with a variable time delay between the two pulses. The results of these calculations are shown in
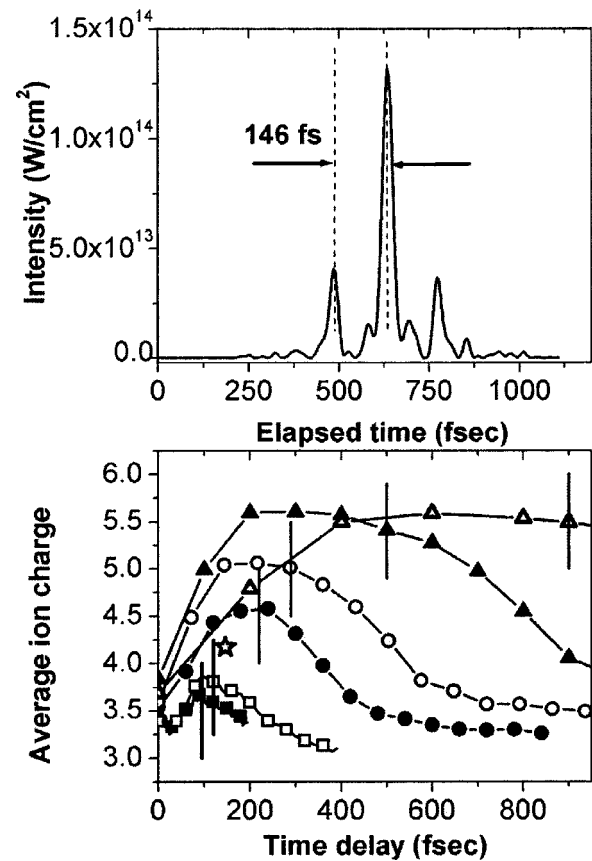

FIG. 3. (a) Optimal pulse shape found in an optimal-control calculation for the ionization of Xe$_{108}$ by a tailored laser pulse derived from a 30 fs, 3.5×10^{14} W/cm^2 laser pulse. Efficient ionization is achieved by a sequence of two pulses separated by 146 fs; (b) average ionic charge-state resulting from the interaction of a sequence of two 30 fs, 1.75×10^{14}W/cm^2 Gaussian pulses with Xe$_n$ clusters, where $n = 64$ (solid squares), 108 (open squares), 302 (solid circles), 588 (open circles), 1524 (solid triangles), and 5056 (open triangles). The result of the optimal-control calculation given in (a) is shown as a star. The vertical lines indicate the times where the electron density n_e of the plasma generated by the first pulse falls to $3n_{crit}$. Very good agreement is observed between this time delay and the optimum delay between the two pulses.

Fig. 3(b). For every cluster size an optimum delay between the two pulses was found that produced a higher average charge-state than the FTL pulse. By monitoring the electron density in the cluster as a function of time delay, we could determine that this optimum corresponds to the time delay where the second pulse interacts with the cluster around the time that the electron density density n_e dropped to $3n_{crit}$. In other words, the simulations provide considerable evidence for the notion that the optimal pulse shape found in our experimental studies using $\langle N \rangle = 1.6 \times 10^4$ atoms/cluster and in our numerical studies using several hundred atoms/cluster reflects a resonance enhancement as suggested by a nanoplasma description of the laser-cluster dynamics. In the two-pulse sequence, the first pulse initiates the plasma formation and the expansion of the cluster. However, during the excitation the electron density rapidly rises above $3n_{crit}$, reducing the efficiency of the energy deposition. Maximum energy

deposition is achieved when further excitation is delayed until the electron density becomes low enough, which in the experiment occurs after about 500 fs. In further support of this interpretation, we have experimentally observed that the optimum time delay for the formation of highly charged ions depends on the laser intensity and the cluster expansion conditions. Upon increasing the laser intensity a shortening of the optimum time delay was observed, consistent with a more rapid cluster expansion. Conversely, using a conical nozzle, clusters with 100 times more xenon atoms could be produced and—consistent with the slower expansion of these larger clusters—an optimal delay of 3.3 ps was found [see the resulting autocorrelation trace in Fig. 2(b)]. Similar cluster-size effects have been observed in experiments where cluster explosions were investigated by means of detection of laser absorption [17], ion energies [8] and transient polarizability [19]. The existence of an optimal time delay for the energy deposition is also consistent with experiments on the production of energetic electrons [10,11] using a variable-pulse-length laser and pump-probe experiments on the production of multicharged [20] and energetic ions [21].

In conclusion, we have presented optimal-control experiments and calculations that provide strong support for the resonance enhancement suggested by the nanoplasma model of cluster ionization. We have shown both experimentally and numerically that there exists a specific time when the laser field is most efficiently coupled to the electrons in the cluster, and have observed in our numerical simulations that the optimum delay of the second laser pulse approximately corresponds to the time where the electron density n_e in the cluster has fallen to $3n_{crit}$. The fact that we have two well-separated pulses indicates that in the time interval between the two pulses any available laser field interacts poorly with the cluster, since the density of free electrons leads to a screening of the laser field [22]. A detailed interpretation of the mechanism of the resonant enhancement will be the subject of a future publication [23].

[1] T. Ditmire, R. A. Smith, J. W. G. Tisch, and M. H. R. Hutchinson, Phys. Rev. Lett. **78**, 3121 (1997).

[2] T. Ditmire, J. W. G. Tisch, E. Springate, M. B. Mason, N. Hay, R. A. Smith, J. Marangos, and M. H. R. Hutchinson, Nature (London) **386**, 54 (1997).

[3] T. Ditmire, J. Zweiback, V. P. Yanovsky, T. E. Cowan, G. Hays, and K. B. Wharton, Nature (London) **398**, 489 (1999).

[4] I. Last and J. Jortner Phys. Rev. A **62**, 013201 (2000).

[5] C. Rose-Petruck, K. J. Schafer, K. R. Wilson, and C. P. J. Barty, Phys. Rev. A **55**, 1182 (1997).

[6] C. Siedschlag and J. M. Rost, Phys. Rev. Lett. **89**, 173401 (2002).

[7] T. Ditmire, T. Donnelly, A. M. Rubenchik, R. W. Falcone, and M. D. Perry, Phys. Rev. A **53**, 3379 (1996).

[8] E. Springate, N. Hay, J. W. G. Tisch, M. B. Mason, T. Ditmire, M. H. R. Hutchinson, and J. P. Marangos, Phys. Rev. A **61**, 063201 (2000).

[9] Y. L. Shao, T. Ditmire, J. W. G. Tisch, E. Springate, J. P. Marangos, and M. H. R. Hutchinson, Phys. Rev. Lett. **77**, 3343 (1996).

[10] E. Springate, S. A. Aseyev, S. Zamith, and M. J. J. Vrakking, Phys. Rev. A **68**, 053201 (2003).

[11] V. Kumarappan, M. Krishnamurthy, and D. Mathur, Phys. Rev. A **66**, 033203 (2002).

[12] R. S. Judson and H. Rabitz, Phys. Rev. Lett. **68**, 1500 (1992).

[13] O. F. Hagena, Rev. Sci. Instrum. **63**, 2374 (1992).

[14] A. T. J. Eppink and D. H. Parker, Rev. Sci. Instrum. **68**, 3477 (1997).

[15] See, D. E. Goldberg, *Genetic Algorithms in Search Optimization and Machine Learning*, 20th ed. (Addison-Wesley Longman, Reading, MA, 1999), for an introduction to simple genetic algorithms and an explanation of the parameters used in the optimization.

[16] M. A. Klosner and W. T. Silfvast, Opt. Lett. **23**, 1609 (1998).

[17] J. Zweiback, T. Ditmire, and M. D. Perry, Phys. Rev. A **59**, R3166 (1999).

[18] E. S. Toma and H. G. Muller, Phys. Rev. A **66**, 013204 (2002).

[19] K. Y. Kim, I. Alexeev, E. Parra, and H. M. Milchberg, Phys. Rev. Lett. **90**, 023401 (2003).

[20] E. M. Snyder, S. A. Buzza, and A. W. Castleman, Jr., Phys. Rev. Lett. **77**, 3347 (1996).

[21] E. Springate, N. Hay, J. W. G. Tisch, M. B. Mason, T. Ditmire, J. P. Marangos, and M. H. R. Hutchinson, Phys. Rev. A **61** 044101 (2000).

[22] We want to draw attention to recent papers that corroborate the results reported in this paper, namely, U. Saalmann and J. M. Rost, Phys. Rev. Lett. **91**, 223401 (2003); and C. Jungreuthemayer, M. Geissler, J. Zanghellini, and Th. Brabec, *ibid.* **92**, 133401 (2004).

[23] T. Martchenko, S. Zamith, C. Siedschlag, H. G. Muller, and M. J. J. Vrakking (unpublished).